Bulletin of Environment, Pharmacology and Life Sciences
Bull. Env. Pharmacol. Life Sci., Vol 12 [2] January, 2023: 149-157

Online ISSN 2277-1808
Journal's URL:http://www.bepls.com
CODEN: BEPLAD

ORIGINAL ARTICLE **OPEN ACCESS**

Green Synthesis and Characterization of Silver Nanoparticles Using Flowers of *Russelia equisetiformis* Extract and their Anticancer Activity on MCF-7 Cell Lines

Yashraj Yadav*, Deshraj Chumbhale
Faculty of Pharmacy, Oriental University, Indore, Madhya Pradesh, India.
***Correspondence E-mail**- yashrajyadav@gmail.com

ABSTRACT

In 2020, there will be 2.3 million new instances of breast cancer detected in women worldwide, with 685 thousand deaths. It is estimated that by the end of 2020, 7.8 million women will still be alive who have been diagnosed with breast cancer in the previous five years, making it the most common type of cancer worldwide. The predicted number of new cases of breast cancer is increasing every month. By treating silver ions with an extract of Russelia equisetiformis flowers, silver nanoparticles (NPs) were quickly created to evaluate their in-vitro anticancer activity. Green nanoparticles were created using a hydroalcoholic extract of Russelia equisetiformis (HERE) flowers, which were then characterized using UV/vis spectrophotometry, Fourier-transform (FT) infrared spectrophotometry, scanning electron microscopy (SEM), energy-dispersive X-ray (EDX) analysis, X-ray diffraction (XRD), and cytotoxicity (MTT assay). The generated silver nanoparticles (AgNPs) were discovered to be crystalline and spherical, with sizes ranging from 40 to 90 nm. The HERE-AgNPs generated were cytotoxic to MCF-7, with an inhibitory concentration (IC50) of 21.38 g/mL. Russelia equisetiformis flower-based bio-fabricated nanoparticles show antitumor action.

Keywords: *Russelia equisetiformis, silver nanoparticles, anticancer activity, MTT assay*

Received 21.08.2022 Revised 15.11.2022 Accepted 18.12.2022

INTRODUCTION

Cancer has spread its roots all across the world, including India, in recent decades. Cancer is not just a disease, but it is also the top cause of death worldwide. There are various types of cancer, with breast cancer being one of the most common. According to WHO, the total number of new cases in 2020 will be 19292789, with breast cancer accounting for the greatest number of new cases (11.7 percent), while the total number of fatalities in 2020, both sexes and all ages, will be 9958133. India is the third-largest country in terms of cancer mortality and incidence (after China and the United States). The projected number of new cases of breast cancer in India in 2020 is 2261419[1]. Cancer is a complex disease in which cells in a given tissue or region no longer respond to the signals that control cellular differentiation, survival, proliferation, and death within the tissue. Instead of dying, aged cells proliferate uncontrollably, resulting in the formation of neoplasms, or abnormal cells, in the body. Tumors are tissue masses that form when extra cells combine to form a mass of tissue. It is important to note, however, that the original human cell is not always connected with the cancerous stem cell, which is a cellular fraction inside the tumor engaged in the specific maintenance of malignant growth. In other words, progenitor cells and CSCs are cells that start cancer and cells that spread cancer, respectively [2]. All ductal carcinomas originate near or within the TDLU (terminal duct lobular unit), which induces an epithelial layer and is separated from the stromal tissue, which is made up of lymphocytes, myofibroblasts, macrophages cells, fibroblasts, mast cells, and neutrophils cells, as well as the basement membrane. Breast cancer is the most frequent kind of cancer among women of reproductive age. The oncogene becomes activated and transforms cancer cells into ductal solid tumors [3]. Ayurvedic medicine is one of the oldest and most well-known medical systems in India. Numerous drugs are based on a metal and mineral composition known as Bhasma, which is commonly utilized in India, in this technique. The production processes used by Bhasma are in line with modern nanotechnology, and the nanocrystalline materials produced are physiochemically identical to one another. They include a variety of minerals that contain important minerals and elements such as calcium, potassium sodium, and manganese, as well as other minerals like zinc with copper, silver metal (Rajat bhasma), iron metal (loh bhasma) swarn, or gold Bahama, etc [4]. Nanoparticles can easily penetrate cells and participate in cellular metabolism, DNA/protein interaction,

and gene expression, with the ability to modify gene expression. AgNPs (silver nanoparticles) have significant therapeutic potential due to their ability to induce apoptosis via a variety of mechanistic pathways, including mitochondrial dysfunction, DNA splitting, cell membrane disruption, impairment of cellular signalling pathways, altered enzyme activity, and the formation of reactive oxygen species [5]. AgNPs produced in a green environment produce reactive oxygen species (ROS), which eventually cause cell death. ROS generation harms signal transduction pathways, resulting in cell death. The generation of hydrogen peroxide on mitochondrial membrane potential leads to the dissociation of respiration from the rest of the body. AgNPs promote ROS formation and a drop in glutathione (SGH) levels after entering the cell, as well as the activation of nuclear factor-kB (NF-kB) and tumor necrosis factor-alpha (TNF-alpha). Increased superoxide radicals impair mitochondrial transmembrane potential and disrupt the signal transduction pathway, both of which cause apoptosis and cell death [6,7]. AgNPs produce reactive oxygen radicals (ROR) in a green environment, which cause cell death. ROS production disrupts signal transduction pathways, resulting in cell death. Hydrogen peroxide's effect on mitochondrial membrane potential decouples oxygen from the rest of the body. When AgNPs enter the cell, they induce ROS generation, a decrease in SGH levels, and the activation of NF-kB and TNF-alpha (TNF-alpha). Increased superoxide radicals affect mitochondrial transmembrane potential and the signal transduction system, resulting in apoptosis and cell death [6,7]. Increased ROS levels and decreased GSH levels affect biological components such as DNA, lipid membrane peroxidation, and protein carbonylation (protein harmful oxidation). A wide range of plant-derived metabolites can target molecular and cellular pathways involved in the Etiology of diseases like cancer and metabolic syndrome. Despite its disadvantages, plant-based nanoparticle synthesis has proven to be a viable and efficient method of manufacturing cost-effective and ecologically friendly nanoparticles. The use of plant extracts has various advantages, one of which is that there is no issue in maintaining or conserving the culture medium, which is an important operation in microbiological culture. A large-scale plant-mediated biosynthesis of the nanoparticle could be achieved with no pollutants introduced [8].Nanomaterial Characterization Understanding and regulating nanoparticle manufacturing and applications is critical for understanding and controlling nanoparticle characteristics. Size and shape are two of the most essential characteristics of NPs. Surface charge, area, size, and degree of aggregation can all be quantified. investigate the surface chemistry Fourier transformations Some of the techniques used to evaluate nanoparticles include infrared spectroscopy (FTIR), X-ray photoelectron spectroscopy (XPS), atomic force microscopy (AFM), powder X-ray diffractometry (XRD), dynamic light scattering (DLS), and ultraviolet-visible spectroscopy (UV-Vis). These methods can be used to calculate particle size, morphology, crystallinity, fractal dimensions, pore diameter, and surface area. The value of TEM is that it examines 3D images and measures particle height and diameter. Calculating the volume is required. The grape represents the particle size distribution. Dynamic light scattering was also employed to identify. Furthermore, X-ray diffraction is used to assess crystallinity, and UV-visible light is used to detect colour. To validate sample formation, visible spectroscopy is used [9]. Nanoparticles are now being used in a range of healthcare systems as nanotechnology and other sectors of nanotechnology advance. Nanomedicine has already proven to help treat chronic infections and SARS-like disorders, among other uses, due to the use of drug delivery systems and nanosensors. Nanomedicine and its components have the potential to make a significant difference in preventive medicine, diagnosis, therapy, immunization, and scientific investigation. Biosensors based on nanomaterials such as quantum dots can detect sickness and make medical diagnoses. Plants' metal nanoparticles are significantly more stable than other species' metal nanoparticles. Plants (and especially plant extracts) can deplete metal ions faster than fungus or bacteria. Nanotechnology provides advantages and aids in the overall increase of pharmacological therapeutic qualities by employing nano-systems such as polymeric, liposomes, lipid, and metallic nanoparticles, and micelles for drug encapsulation [10].

MATERIAL AND METHODS

Material

Analytical-grade chemicals were used throughout. Loba Chemical Pvt. Ltd. provided the silver nitrate (AgNO3, 99.8%), and Merck provided the ethanol (Germany). All studies were conducted using deionized and milli-Q water.

Plant material collection and extraction

Russelia equisetiformis flowers were collected from a local garden in Indore [M.P]. Dr. Naveen Kumar Jain, Botanist, Government Holkar (Model, Autonomous) Science College, Indore, Department of Botany (M.P.) India (Voucher no. 01A/Bot.Holker/2020), authenticated the plants. To remove contaminants, all *Russelia equisetiformis* flowers were washed with deionized water and air-dried for 14 days in the shade. Using an electric laboratory blender, the fine, coarse powder was extracted from the dried flowers *of Russelia*

equisetiformis. To complete the extraction in a single phase, cold maceration with ethanol and water in a 70:30 v/v ratio was used. 30 g of powdered material was combined with 100 ml of hydroalcoholic solvent for ten days before being filtered through Whatman filter paper. The sample material was boiled in an electric oven for 45 minutes at 50 degrees Celsius with a magnetic stirrer. The hydroalcoholic extract of *Russelia equisetiformis* (HERE) was cooled and collected dry in a well-closed container. This filtrate was used in the production of plant-based nanoparticles. It was employed as a stabilizer as well as a reducing agent [11, 12].

Phytochemical analysis

According to WHO guidelines [13] and Ayurvedic Pharmacopoeia [14], a small portion of the dry extract of HERE was used for phytochemical tests for compounds such as carbohydrates, proteins, and tannins, phenols, flavonoids, alkaloids, saponins, glycosides, terpenes, and steroids.

Biosynthesis of silver nanoparticles

To make silver nanoparticles, start with a silver nitrate stock solution (0.1M), Using a pipette, dissolve 16.99 gm of silver nitrate in 500 ml distilled water. After 80 mL of AgNO3 (0.1 M) solution, add enough water to make 1000 mL and dissolve 20 mg of extract (*Russelia equisetiformis* hydroalcoholic extract). To avoid silver nitrate photoactivation, the reaction was carried out in the dark. The mixture changed colour from light yellowish-brown to dark reddish-brown after 12 hours of incubation at 37^0 C, indicating silver ion reduction. The nanoparticles were centrifuged at 10,000 rpm for 45 minutes after reduction, and the powder pellet was cleaned three times in water [15].

Characterization of synthesized silver nanoparticles

UV-Vis. spectrophotometer analysis

AgNPs have a distinct set of optical properties that cause them to interact strongly with specific wavelengths of light when exposed to them. Shimadzu UV-Visible Absorption Spectroscopy (Shimadzu UV-1800 UV/Visible) The wavelength range of 300-750 nm has been used to monitor the formation of biogenic AgNPs and the bioreduction of Ag+ ions in solution. This technique provides the result of the metal's surface plasmon resonance. It was used to track the formation of biogenic AgNPs and the bioreduction of Ag+ ions in solution. This phenomenon, known as surface plasmon resonance (SPR), is caused by the interaction of conduction electrons in metal nanoparticles with light photons, which results in a resonance effect. An analysis of UV-visible spectroscopy performed using the Shimadzu-1800 model [16].

FTIR spectroscopy

To verify that various kinds of biomolecules, biochemicals, inorganic materials, surface composition, and ligand binding are all involved in the transformation of silver ions into AgNPs, an FTIR spectrophotometer is utilized. To obtain a resolution of 450–4000 cm-1 for the hydroalcoholic extract of *Russelia equisetiformis* silver nanoparticles (HERE-AgNPs) powder, a Shimadzu FT-IR spectrophotometer was used [17,18].

X-ray diffraction (XRD)

The crystalline nature of AgNPs was demonstrated by the XRD pattern that was obtained from the Panalytical Empyrean X-ray diffractometer located at IISER in Bhopal, Madhya Pradesh, in the 2teta range from 20 to 80 degrees. Casting silver nanoparticle powder onto a glass slide and allowing it to air-dry at room temperature to create a sample for XRD measurement was the first step in the process. Cu KA radiation obtained a measurement of 1.541874 when it was applied to the pattern [19].

Scanning electron microscopy (SEM)

The scanning electron microscope (SEM) approach was utilized to verify the surface morphology and topography of the generated silver nanoparticles. The examination of the HERE-AgNPs that took place at CIF, IISER, Bhopal, MP [20] was carried out using a high-resolution field emission scanning electron microscope (HR FESEM) made by Zeiss and given the model's name ULTRA Plus.

Energy-dispersive X-ray (EDX) analysis

The Oxford Nanoanalysis Instruments and the high-resolution transmission electron microscope were used for energy-dispersive X-ray (EDX) analysis to confirm the presence of silver in the particles as well as to discover other elementary particle compositions [21].

MTT (Cytotoxicity) Assay

Cell viability can be measured using the MTT (cytotoxicity) assay, which has been around for a long time. MTT-formazan is formed by succinate dehydrogenase (mitochondrial complex II) via enzymatic cell reduction of 3-[4,5-dimethylthiazole-2-a]-2,5 diphenyltetrazolium bromide (MTT). It's worth noting that because their mitochondria are dormant, even freshly destroyed cells don't leave much MTT behind. Because MTT cleavage is proportional to the number of living cells present, colorimetric techniques can be used to quantify this quantity. This cell line assay was performed following the standard operating procedures at DP Laboratories in Bhopal. To disperse the chemicals, DMSO was used, and the samples

were serially diluted -in a complete medium until the necessary quantities were reached. The concentration of DMSO (dimethyl sulfoxide) in all samples was kept below 0.1 percent. MCF7 cells cultivated in unsuitable circumstances were plated in 96-well plates and treated with varying concentrations of the test substances before being incubated at 37 degrees Celsius with 5% CO2 for 96 hours. applied the MTT reagent to the wells and incubated them for 4 hours before detecting the dark blue formazan product generated by the cells at 550nm. The percent (percent) of inhibition at each concentration was calculated and shown to obtain the IC50 values [22,23].
To calculate the likelihood of cell death, apply the following equation: (Test OD/Control OD) X 100 equals the viability percentage. The cytotoxicity level is set to 100-Percentage of viability.

RESULTS AND DISCUSSION

Phytochemical screening

An analysis of the phytochemical group was carried out for tannins (determined with the $FeCl_3$ test, the $K_2Cr_3O_7$ test, and the lead acetate test), glycosides (determined with the Legal's test, the Keller-test, Killiani's, and the Borntrager's test), saponins (determined with the foam test), alkaloids (determined with Mayer's test, Dragendorff's test, Wagner's test, and Hager's test), phytosterols (determined with the Liebe (using the $FeCl_3$ test). It is found that, discovered that the hydroalcoholic extract of *Russelia equisetiformis* included polyphenol saponins, cardiac glycoside, triterpenes, tannins, and flavonoids. These chemical compounds might play a significant part in the process of reducing the size of silver ions or transforming them into nanoparticles.

UV–visible spectroscopy

These compounds may play an important role in the reduction or conversion of silver ions to nanoparticles. The colour change from pale yellowish-brown to dark reddish-brown showed a definite peak at 441.7 nm (Figure.1), demonstrating the production of silver nanoparticles using 0.1M silver nitrate solution as a result of metal ion bioreduction by the plant extract.

Fourier-transform infrared spectroscopy (FTIR)

This method has been effectively used to identify the biomolecules involved in the reduction of silver metal ions to silver nanoparticles. It has also been successfully used to correlate FTIR fingerprint data with normal IR fingerprint data. FTIR absorption spectra are a type of absorption spectrum and are shown in Fig 2. A hydroalcoholic extract of *Russelia equisetiformis* silver nanoparticles (HERE-AgNPs) and a hydroalcoholic extract of *Russelia equisetiformis* (HERE) are shown in Fig.2. The strong characteristic band at 3358.68 to 3000 cm^{-1} is assigned to the O–H. This accounts for the presence of alcohol and phenol groups, whereas HERE-AgNPs spectra show a shortened peak at 3286.84 of or N–H stretching of amide or crystal water, which may exhibit the formation of the nanocrystal. The weak band is about 2890.45 to 2348.43cm^{-1} and correspondsto C-H and N=H stretches of alkanes and secondary amines with an aromatic ring [24]. Stretching to C = C of diene, triene, and aromatic systems in the week band 1600 to 1650 cm^{-1}. The peak appears at 1383.98 to 1258.6 and shows starching of CO and CN for carboxylic and amide groups, respectively. The peaks at 1154.45 to 1187.24, 1034 to 1016 cm^{-1} showed ether, ester and haloalkane stretching respectively. The C-H bending in the isolated aromatic group is shown by the absorbance peak at 876–851 cm^{-1}. The Ag-O is associated with weak absorbance bands at 583, 537, and 529 cm-1. The metal-oxygen zone is located between 400 and 600 cm-1[25].

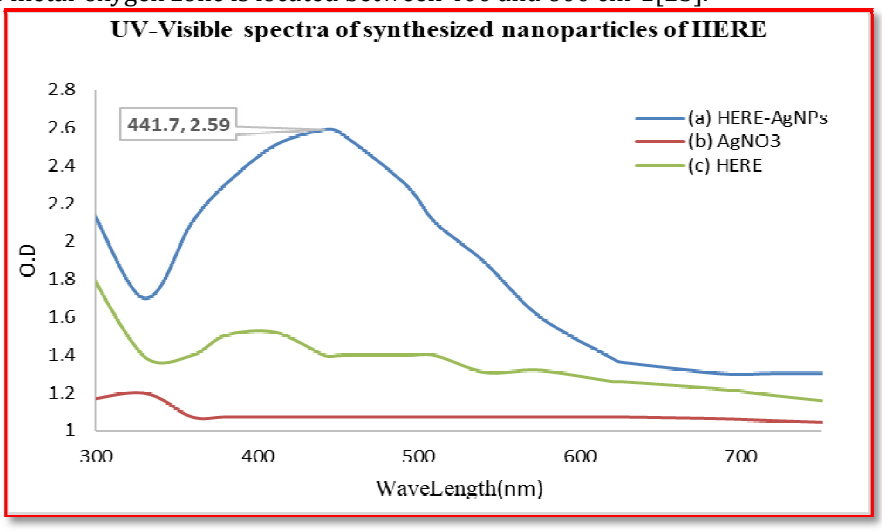

Figure 1: The UV-visible absorption spectrums of HERE-AgNO3 (A), AgNO3 (B), and only HERE (C)

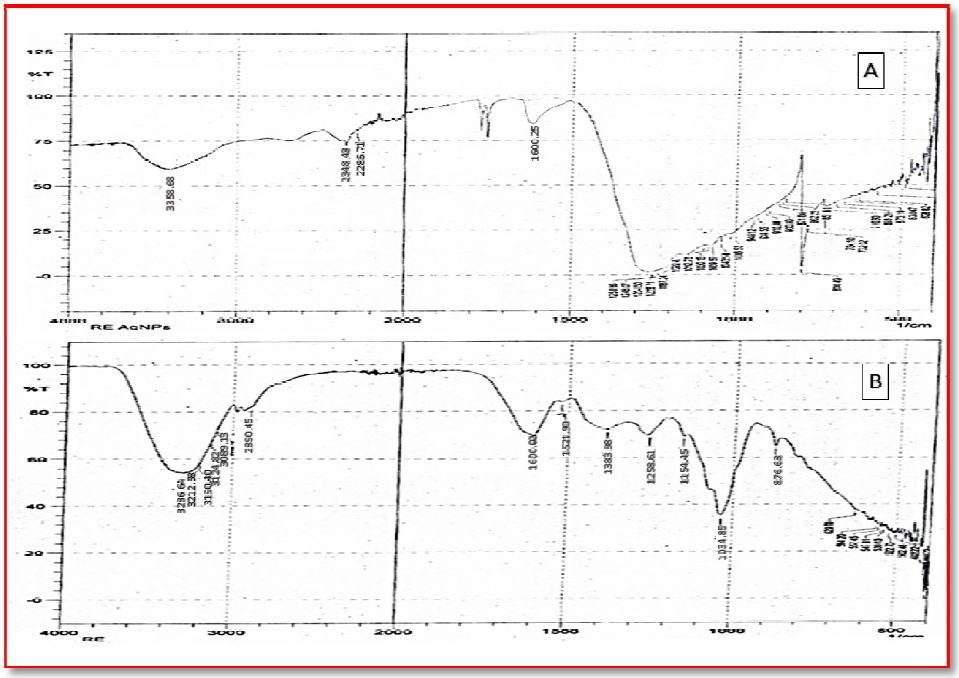

Figure 2: FTIR absorption spectra HERE AgNPs(2A) and HERE(2B)

X-ray diffraction (XRD)

Figure 3, illustrates the XRD pattern, and the crystalline nature was confirmed by comparing the peak of silver nanoparticles of HERE-AgNPs to the crystal database (the degree of structural order of a solid is 100 percent, and the amorphous phase is 0 percent). The four distinct diffraction peaks occur at 2 theta values of 37.62, 46.37, 64.05, and 75.01, and correspond to Miller index (hkl) values (1 1 1), (2 0 0), (2 2 0), and (2 2 0), respectively (3 1 1). Additional peaks were observed at 32.64, 29.52, 24.18, and 55.21 for silver face-centered cubic structure reflection planes. These peaks were caused by the HERE extract, which is made up of organic compounds from plants and is responsible for the reduction of silver ions (Ag0) and the stability of the resulting nanoparticle [26].

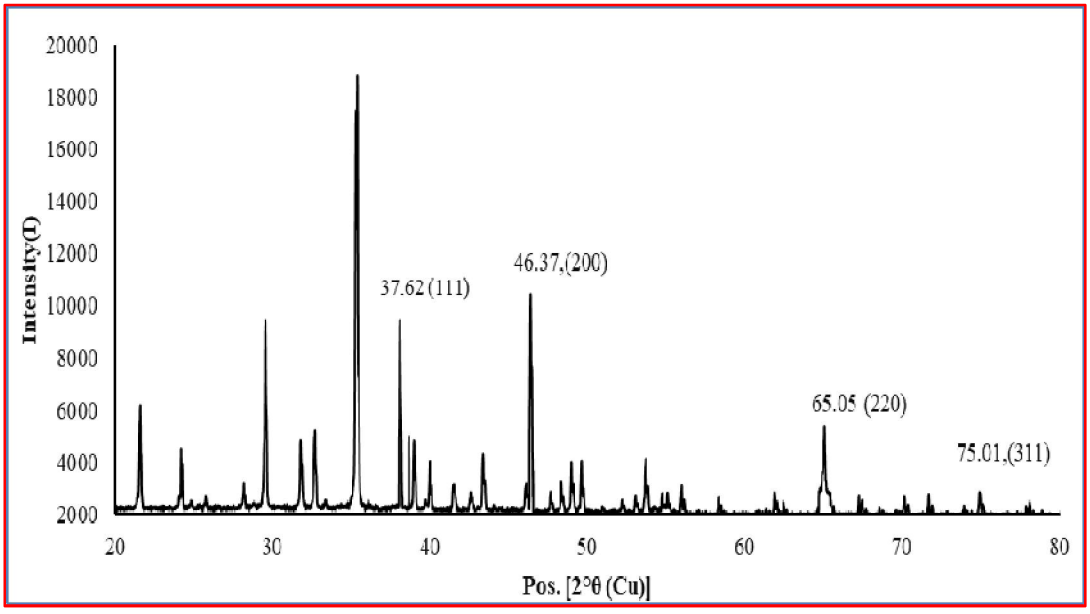

Figure 3: XRD pattern of HERE-AgNPs

Scanning electron microscopy (SEM)

The photomicrographs obtained by scanning electron microscopy (SEM) for use in the morphological analysis are depicted in figures 4a and 4b. Several views of silver nanoparticles formed by RE plant

extract at varying magnifications are presented here. The core particles had a size distribution that ranged from 40.35 to 90.47 nm, as can be seen in Figure 4a. At 10x magnification, the program "ImageJ" was used to locate specific nanostructures that resembled rods and cubes; the particle size determined by this method is almost identical to that obtained by XRD analysis. Nanoparticles and subunits might clump together to form larger particles, which would lead to a significant variation in particle size.

EDX (energy-dispersive X-ray) analysis

In this study, energy descriptive analysis was used to trace the elemental composition and proportional abundance of bio-fabricated HERE-AgNPs due to surface plasmon resonance. Metallic silver nanocrystals typically have an optical absorption peak at around 3 keV. The EDX spectrum in Fig.5 revealed that silver is present in the synthesized silver nanoparticles (HERE-AgNPs) in the form of silver oxide (56.25%). A small amount of carbon was also found in the nano-formulation that was made, but the EDX profile showed that silver was the most important element.

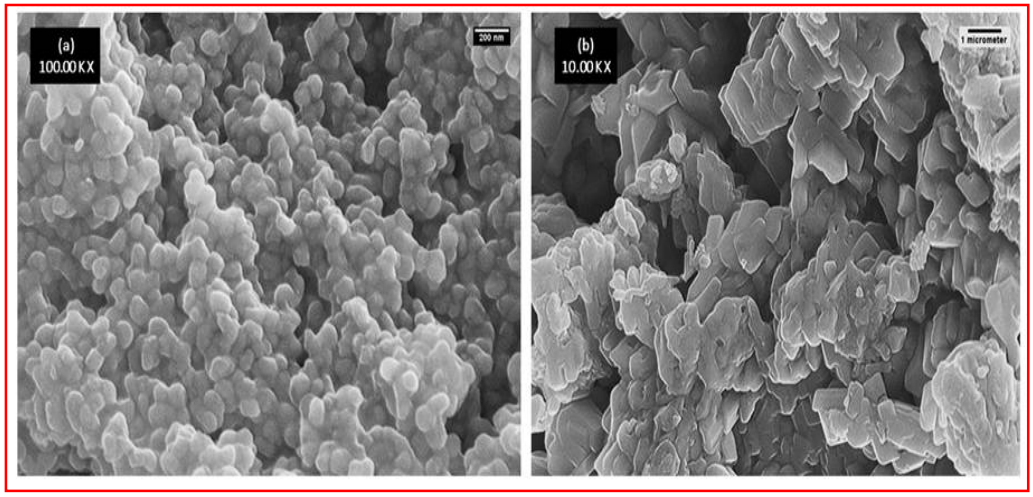

Figures 4a and b: SEM of HERE-AgNPs

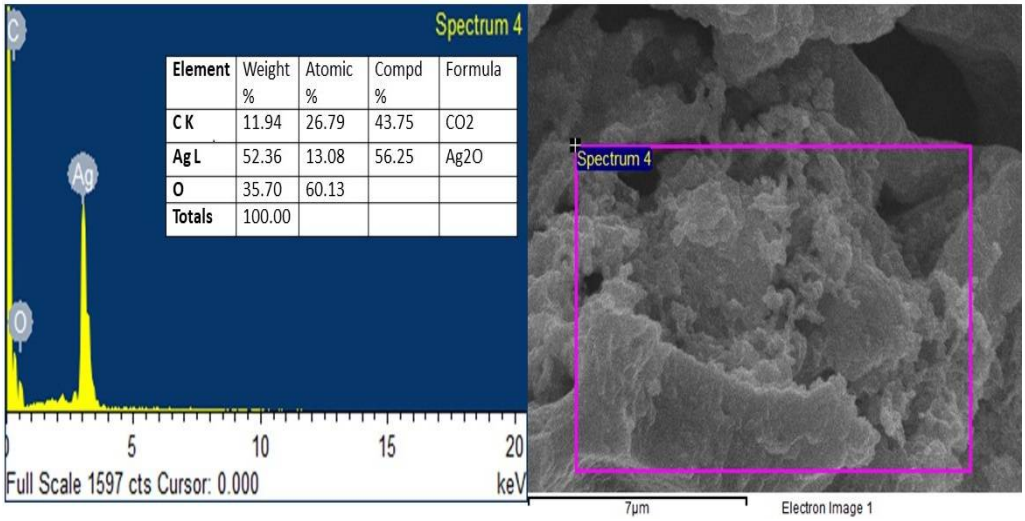

Figure 5: EDX spectrum image and graph of HERE-AgNPs

MTT (Cytotoxicity) Assay

MCF-7 breast carcinoma cells were treated with silver nanoparticles, which were previously formulated. The findings shown in Graph No. 01 demonstrate that the usage of the synthesized HERE-AgNPs at various doses inhibited the proliferation of MCF-7 human breast cancer cells. The AgNPs concentrations utilized ranged from 0.1 g/ml to 60 g/ml, with the lowest concentration being used and the highest being used. In the presence of cancer cells, silver nanoparticles may enter the bloodstream and reach tumor cells via leakage sites in the blood vessels. Graph No. 1 of IC50 values demonstrates that the cytotoxicity of AgNPs is greater than 50% at the lowest concentration (21.38 g/ml). Also, fig.7 shows that inhibition of cell growth in HERE AgNPs is greater than inhibition of cell growth in an untreated breast cancer cell line. This shows that HERE AgNPs can fight cancer.

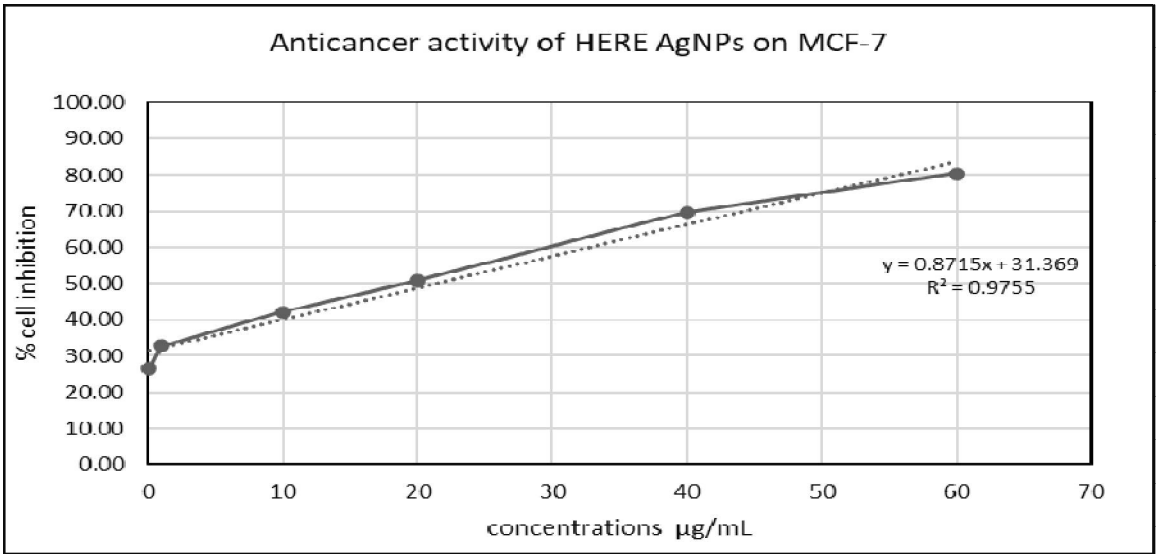

Graph-1: Cytotoxicity of the *HERE-AgNPs* by the MTT assay

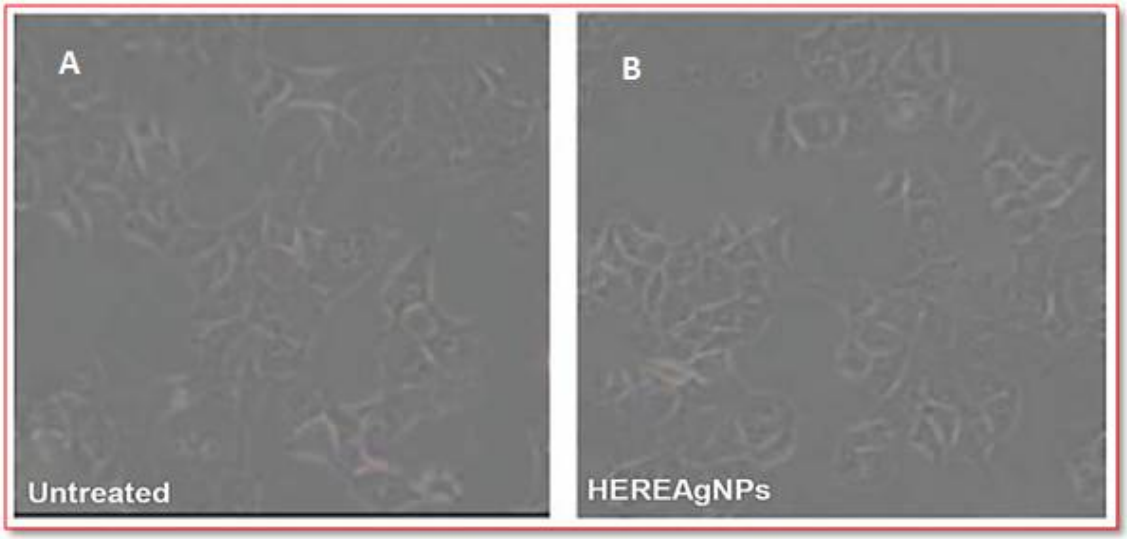

Figure 5: The cellular morphology of (A) untreated MCF-7 cells and (B) HERE-AgNPs treated MCF-7 cells is shown in representative photomicrographs.

CONCLUSION

The current study demonstrated the low-cost and environmentally friendly production of silver nanoparticles for anticancer activity using hydroalcoholic extracts of the *Russelia equisetiformis* species. The hydroalcoholic extract of *Russelia equisetiformis*(HERE) flowers contains polyphenols, flavonoids, and other phytochemicals that act as reducing and capping agents in *Russelia equisetiformis*green production of silver nanoparticles. The silver nanoparticles were all 40 nm in size and spherical in shape, but some of them were agglomerated. Silver nanoparticles were also found to have anticancer activity in this study, which was confirmed by the MTT (Cytotoxicity) assay in the MCF-7 cell line. To better understand the pharmacological and therapeutic potential of this plant (*Russelia equisetiformis* silver nanoparticles), more detailed cell studies and in vivo or animal studies were required.

ACKNOWLEDGMENT

The author would like to thank the people in charge of the labs at IISER, Bhopal (XRD, EDX, SEM), Dashpende lab, Bhopal (MTT assay), and Anusandhan Laboratories, Indore (MP), for making sure that the study could be done.

CONFLICT OF INTEREST

We declare that we do not have any competing interests.

SOURCE OF FUNDING
There is no funding. (self-fund)

REFERENCES

1. Sung, H., Ferlay, J., Siegel, R. L., Laversanne, M., Soerjomataram, I., Jemal, A., & Bray, F. (2021). Global cancer statistics 2020: GLOBOCAN estimates of incidence and mortality worldwide for 36 cancers in 185 countries. *CA: a cancer Journal For Clinicians*, *71*(3), 209-249.
2. Visvader, J. E. (2011). Cells of origin in cancer. *Nature*, *469*(7330), 314-322.
3. Boix-Montesinos, P., Soriano-Teruel, P. M., Arminan, A., Orzáez, M., & Vicent, M. J. (2021). The past, present, and future of breast cancer models for nanomedicine development. *Advanced drug delivery reviews*, *173*, 306-330.
4. Khan, M. S. A., & Ahmad, I. (2019). Herbal medicine: current trends and future prospects. In *New look to phytomedicine* (pp. 3-13). Academic Press.
5. Jabeen, S., Qureshi, R., Munazir, M., Maqsood, M., Munir, M., Shah, S. S. H., & Rahim, B. Z. (2021). Application of green synthesized silver nanoparticles in cancer treatment—a critical review. *Materials Research Express*, *8*(9), 092001.
6. Fani, S., Kamalidehghan, B., Lo, K. M., Nigjeh, S. E., Keong, Y. S., Dehghan, F., ... & Hashim, N. M. (2016). Anticancer activity of a monobenzyltin complex C1 against MDA-MB-231 cells through induction of apoptosis and inhibition of breast cancer stem cells. *Scientific reports*, *6*(1), 1-15.
7. Nishanth, R. P., Jyotsna, R. G., Schlager, J. J., Hussain, S. M., & Reddanna, P. (2011). Inflammatory responses of RAW 264.7 macrophages upon exposure to nanoparticles: role of ROS-NFκB signaling pathway. *Nanotoxicology*, *5*(4), 502-516.
8. Kaur, P., Thakur, R., & Chaudhury, A. (2016). Biogenesis of copper nanoparticles using peel extract of Punica granatum and their antimicrobial activity against opportunistic pathogens. *Green Chemistry Letters and Reviews*, *9*(1), 33-38.
9. Tang, C. Y., & Yang, Z. (2017). Transmission electron microscopy (TEM). In *Membrane characterization* (pp. 145-159). Elsevier.
10. Bhardwaj, K., Dhanjal, D. S., Sharma, A., Nepovimova, E., Kalia, A., Thakur, S., ... & Kuča, K. (2020). Conifer-derived metallic nanoparticles: Green synthesis and biological applications. *International Journal of Molecular Sciences*, *21*(23), 9028.
11. Hernández-Jiménez, A., Kennedy, J. A., Bautista-Ortín, A. B., & Gómez-Plaza, E. (2012). Effect of ethanol on grape seed proanthocyanidin extraction. *American Journal of Enology and Viticulture*, *63*(1), 57-61.
12. Yadav, Y., Mohanty, P. K., & Kasture, S. B. (2011). Anti-inflammatory activity of hydroalcoholic extract of Quisqualis indica Linn. flower in rats. *International Journal of Pharmacy & Life Sciences*, *2*(8).
13. WHO, G. (1998). Quality control methods for medicinal plant material.
14. Mukherjee, P. K., Nema, N. K., Venkatesh, P., & Debnath, P. K. (2012). Changing scenario for promotion and development of Ayurveda–way forward. *Journal of ethnopharmacology*, *143*(2), 424-434.
15. Azkiya, N. I., Masruri, M., & Ulfa, S. M. (2018). Green synthesis of silver nanoparticles using extract of Pinus merkusii Jungh & De Vriese cone flower. In *IOP Conference Series: Materials Science and Engineering* (Vol. 299, No. 1, p. 012070). IOP Publishing.
16. Gomes, H. I., Martins, C. S., & Prior, J. A. (2021). Silver nanoparticles as carriers of anticancer drugs for efficient target treatment of cancer cells. *Nanomaterials*, *11*(4), 964.
17. Gomathi, M., Rajkumar, P. V., Prakasam, A., & Ravichandran, K. (2017). Green synthesis of silver nanoparticles using Datura stramonium leaf extract and assessment of their antibacterial activity. *Resource-Efficient Technologies*, *3*(3), 280-284.
18. Carmo, I. A. D., de Souza, A. K. N., Fayer, L., Munk, M., de Mello Brandão, H., de Oliveira, L. F. C., ... & de Souza, N. L. G. D. (2022). Cytotoxicity and bactericidal activity of alginate/polyethylene glycol films with zinc oxide or silicon oxide nanoparticles for food packaging. *International Journal of Polymeric Materials and Polymeric Biomaterials*, 1-12.
19. Ajitha, B., Divya, A., Harish, G., & Sreedhara Reddy, P. (2013). The influence of silver precursor concentration on size of silver nanoparticles grown by soft chemical route. *Res J Phys Sci*, *2320*, 4796.
20. Krishnaraj, C., Jagan, E. G., Rajasekar, S., Selvakumar, P., Kalaichelvan, P. T., & Mohan, N. J. C. S. B. B. (2010). Synthesis of silver nanoparticles using Acalypha indica leaf extracts and its antibacterial activity against water borne pathogens. *Colloids and Surfaces B: Biointerfaces*, *76*(1), 50-56.
21. Vigneshwaran, N., Kathe, A. A., Varadarajan, P. V., Nachane, R. P., & Balasubramanya, R. H. (2006). Biomimetics of silver nanoparticles by white rot fungus, Phaenerochaete chrysosporium. *Colloids and Surfaces B: Biointerfaces*, *53*(1), 55-59.
22. Martin, A., & Clynes, M. (1993). Comparison of 5 microplate colorimetric assays for in vitro cytotoxicity testing and cell proliferation assays. *Cytotechnology*, *11*, 49-58.
23. Hilger, I., Frühauf, S., Linß, W., Hiergeist, R., Andrä, W., Hergt, R., & Kaiser, W. A. (2003). Cytotoxicity of selected magnetic fluids on human adenocarcinoma cells. *Journal of magnetism and magnetic materials*, *261*(1-2), 7-12.
24. Salleh, A., Naomi, R., Utami, N. D., Mohammad, A. W., Mahmoudi, E., Mustafa, N., & Fauzi, M. B. (2020). The potential of silver nanoparticles for antiviral and antibacterial applications: A mechanism of action. *Nanomaterials*, *10*(8), 1566.
25. Nabavi, S. M., Ebrahimzadeh, M. A., Nabavi, S. F., Hamidinia, A., & Bekhradnia, A. R. (2008). Determination of antioxidant activity, phenol and flavonoids content of Parrotia persica Mey. *Pharmacologyonline*, *2*(9), 560-567.

26. Sharma, P., Dube, B., & Sawant, K. (2011). Development and evaluation of nanostructured lipid carriers of cytarabine for treatment of meningeal leukemia. *Journal of nanoscience and nanotechnology*, *11*(8), 6676-6682.

CITATION OF THIS ARTICLE

Yashraj Yadav, Deshraj Chumbhale. Green Synthesis and Characterization of Silver Nanoparticles Using Flowers of *Russelia equisetiformis* Extract and their Anticancer Activity on MCF-7 Cell Lines. Bull. Env. Pharmacol. Life Sci., Vol 12[2] Jan 2023: 149-157.